ISSN 1392–1207. MECHANIKA. 2023 Volume 29(1): 59–66

Research on Intelligent Formation Operation Performance of Straddle-Type Rapid Transit Vehicles in Heterogeneous Operating Environment

Zixue DU*, Haoxin WU, Zhen YANG***, Xiaoxia WEN******

**Institute of Urban Rail, Chongqing Jiaotong University, 400074 Chongqing, P.R. China, E-mail: aaadzx@163.com*
***Institute of Urban Rail, Chongqing Jiaotong University, 400074 Chongqing, P.R. China,*
E-mail: 15310165464@163.com (Corresponding author)
****Institute of Urban Rail, Chongqing Jiaotong University, 400074 Chongqing, P.R. China, E-mail: 21930315@qq.com*
*****Institute of Urban Rail, Chongqing Jiaotong University, 400074 Chongqing, P.R. China,*
E-mail: 963884811@qq.com

crossref http://dx.doi.org/10.5755/j02.mech.32110

1. Introduction

After a period of rapid development and construction of urban rail transit lines, some cities in China have to consider the high costs of urban rail transit operation and maintenance, which increase the financial burden of local governments. With the introduction of a series of national policies, the central government's restrictions on the construction of urban rail transit lines are also increasing layer by layer. For many cities in China, there is still a demand to build urban rail transit lines, expecting urban rail transit lines with independent right of way to solve the increasingly serious traffic congestion problem. Therefore, many research institutions and enterprises are looking for new urban rail transit solutions. In order to reduce the construction, operation and maintenance costs of urban rail transit lines, and to seize the huge blue ocean market of urban rail transit construction in third and fourth tier cities in China, they are designing a new standard urban rail transit system suitable for small and medium-sized urban rail transit lines, airport connecting lines, and tourist lines.

In this context, on the basis of the team's research on Chongqing straddle monorail Line 3 for many years, we proposed a straddle-type rapid transit formation vehicle operating in IFOM, and carried out a series of preliminary studies [1]. Through the use of vehicle-to-vehicle (V2V) communication and advanced sensors, vehicles operating in IFOM can operate in formation without physical coupler. According to the passenger flow, the vehicle can adopt the single vehicle operation mode (SVOM) or IFOM. Hence, according to the passenger flow demand of the line, the vehicles operating in SVOM can be grouped into formation, and the vehicles operating in IFOM can be split into vehicles operating in SVOM to adapt to the changing passenger flow at any time.

Vehicle platooning has been studied for a long time, and virtual coupling (VC) has also become a popular direction in recent years. The concept of VC is a method proposed by Bock U et al. to improve the utilization rate of lines. Afterwards, they proposed the design and development method of VC on freight railways [2].

In terms of the train formation cooperative control method and control algorithm, in order to solve the speed limit calculation in VC and train safety control when overspeed occurs, the calculation methods of limit speed difference based on relative coordinates and a collision mitigation approach by minimizing the relative kinetic energy are proposed [3]. Moreover, a variety of model predictive control algorithms are used to construct VC controllers to study cruise control of virtual coupled train sets (VCTS), proving that VC can reduce train spacing while ensuring train safety [4-5]. After that, the artificial potential field method was also used for formation control, which was fused with reinforcement learning algorithm, and it was found that VCTS could converge quickly and precisely control [6].

Relevant research also includes the formation running performance of VCTS. Some studies have used control effects, parking accuracy, formation punctuality, comfort and safety to analyze the operational performance of VCTS [7]. Based on the acceleration and spacing errors, the formation stability has been analyzed [8].

The above objects on VC focus on high-speed railways, freight railways and subway trains driven by steel wheels and rails, and lack of research on urban rail transit vehicles driven by rubber wheels with stronger acceleration and deceleration capabilities. The running mechanism of the bogie used in this study is similar to the bogie of the straddle-type monorail vehicle. The related research mainly focuses on the analysis and optimization of the dynamic performance of the straddle-type monorail vehicle, the tire model and the wear optimization of the running wheel. ADAMS and mode-FRONTIER were used to build an optimization model to optimize the curves performance, comfort and tire partial wear of the single-axle straddle-type monorail vehicle through [9].

At the application level, it can be found that the research object of VC has not yet involved new rail transit vehicles. Due to the limitation of the length of vehicles and platforms, it is difficult for VCTS to enter the station at the same time, which may reduce the operation efficiency. However, those vehicles with shorter vehicle lengths and stronger braking capabilities are more suitable for VC technology, such as straddle-type rapid transit vehicles.

At the research level, the vehicle models in most studies on VC are relatively simple, and the simulated track lines are mostly straight lines, which lack consideration for the different operating environments of each vehicle. At the same time, the simplified vehicle model is difficult to analyze the driving safety and riding comfort of the vehicle, and cannot analyze the impact of vehicle heterogeneity. In addition, the current research is mostly aimed at energy saving, time saving, safety, etc., and the analysis lacks the consideration of vehicle comfort, while in the actual vehicle operation, the riding comfort of the vehicle is a point that must

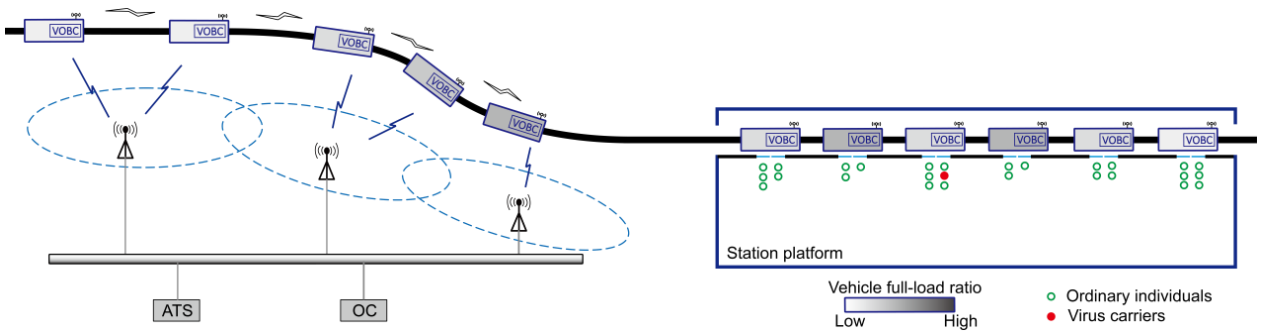

Fig. 1 Architecture of straddle-type rapid transit vehicle operation control system

be considered.

This paper takes the straddle-type rapid transit vehicles operating in IFOM as the object. Firstly, the operation mode of straddle-type rapid transit vehicles is introduced, and the evaluation index system of formation vehicles is proposed according to the heterogeneity of the operation environment of formation vehicles. Then, refer-ring to the vehicle longitudinal dynamics model and the artificial potential field formation algorithm, the formation vehicle operation controller is established. Afterwards, based on the vehicle dynamics model, a multi-rigid body dynamics simulation model of formation vehicles in a heterogeneous operating environment is constructed. Finally, according to the actual operation scenarios of the formation vehicle, the operation performance of the formation vehicle in the heterogeneous operation environment is analyzed.

2. Operation mode

The straddle-type rapid transit vehicle operates within the vehicle operation control system architecture. The vehicle operation control system includes automatic train supervision (ATS), object control (OC), vehicle onboard controller (VOBC) and communication system, etc. The architecture of the vehicle control system is shown in Fig. 1.

The operation control center (OCC) of the line network can plan and schedule the vehicles on the line according to the real-time passenger flow forecast data of each line and the daily operation plan, so as to specify the operation mode for each vehicle. Then the ATS sends the operation command to each vehicle, and the OC manages the switch and the track-side equipment. Finally, after the vehicle receives the task command through the vehicle-ground communication, VOBC can integrate the V2V communication and sensor data to calculate the speed curve of the vehicle autonomously.

We believe that line capacity needs to be adjusted when real-time passenger flow forecast data does not match line capacity. This concept can be expressed as:

$$\left|K_p - K_c\right| > K_q, \tag{1}$$

where: *Kc* is the one-way real-time capacity coefficient; *Kp* is the one-way passenger flow coefficient in the next 15 minutes; *Kq* is the adjustment coefficient; *Kc* and *Kp* are proportional to the passenger flow and capacity respectively. The judgment logic of the vehicle operating mode can be represented as Fig. 2.

When the capacity of the line is saturated, the vehicles can be operated in SVOM, and the redundant vehicles can be parked in the turn back line or in the depot. When the capacity of the line is insufficient, vehicles can be operated in IFOM, and use the Inactive vehicle in the turn back line or the depot to participate in the operation.

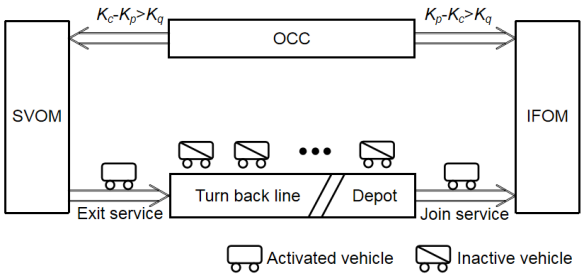

Fig. 2 The judgment logic of the vehicle operating mode

It can be seen that the new operation mode can flexibly match real-time passenger flow and capacity. In addition, because passengers are in different vehicles, it also reduces the risk of COVID-19 transmission.

3. Evaluation index system

As can be seen from Fig. 1, due to the different loads of each vehicle, the acceleration and braking capabilities of each vehicle will be different when running in formation. Additionally, vehicles may have different speed limits as each vehicle travels on a different curve radius. Therefore, when formation vehicles are running, each vehicle is actually in a heterogeneous operating environment.

Considering the influence of the above heterogeneous operating environment on the operation of formation vehicles, we believe that the evaluation index system of formation vehicles not only needs to consider the influence of the heterogeneous operating environment on the longitudinal operation of vehicles, but also the influence of the vehicle passing curve caused by the heterogeneous opera-ting environment.

Therefore, this article uses formation control effect, longitudinal safety and passenger comfort to evaluate the longitudinal driving performance of formation vehicles, and uses running stability to evaluate the safety performance of vehicles passing through curves.

3.1. Formation control effect

The control effect of the formation has a significant influence on the operational safety and operational efficiency of the formation, which can be expressed by the

speed difference between adjacent vehicles, which is expressed as Eq. (2).

$$K_{vij} = v_j - v_i, \tag{2}$$

where: K_{vij} is the speed difference between adjacent vehicles; v_i and v_j are the speeds of the front and rear vehicles, respectively.

When formation vehicles start, the rear vehicle needs to catch up with the front vehicle as soon as possible, which will affect the longitudinal safety of formation vehicles. Therefore, we hold that K_{vij} needs to meet the following requirements:

$$K_{vijmax+} < L_{safe} / t_{free}, \tag{3}$$

where: $K_{vijmax+}$ is the positive maximum value of K_{vij}; L_{safe} is the minimum safety protection distance; t_{free} is the vehicle emergency braking idle time.

Furthermore, in the cruising phase of formation vehicles, the poor speed follow-up between vehicles will lead to an increase in formation length and affect operational efficiency. Therefore, we believe that K_{vij} also needs to meet the requirements of Eq. (4).

$$K_{vij}^{*} = (n-1)K_{vijmax-}t_s / v_{max}t_s. \tag{4}$$

In the formula, K_{vij}^{*} is the maximum cumulative value of K_{vij}; $K_{vijmax-}$ is the maximum negative value of K_{vij}; n is the maximum number of vehicles in formation; V_{max} is the maximum speed; t_s is the vehicle running time gap. So, $K_{vijmax-}$ can be expressed as:

$$K_{vijmax-} < v_{max} / (n-1). \tag{5}$$

To sum up, K_{vij} can be expressed as:

$$\begin{cases} K_{vij} < L_{safe} / t_s & K_{vij} \geq 0 \\ K_{vij} < v_{max} / (n-1) & K_{vij} < 0 \end{cases}. \tag{6}$$

When L_{safe} = 2 m, t_{free} = 1 s, n = 8, v_{max} = 22 m/s, $k_{vijmax+}$ and $k_{vijmax-}$ are 2 m/s and -3.14 m/s respectively.

3.2. Longitudinal safety

The operation of formation vehicles needs to meet the operation protection strategy of formation vehicles, as shown in Fig. 3. From Fig. 3, the relationship between vehicles can be expressed as:

$$D_{min} + L_{istop} + L_{vehicle} = L_{jstop} + L_{safe} + L_{vehicle}. \tag{7}$$

where: D_{min} is the minimum safe tracking distance of the rear vehicle; L_{istop} and L_{jstop} are the braking distances of the front and rear vehicles respectively; $L_{vehicle}$ is the length of the vehicle. So, the minimum safe tracking distance for the vehicle is:

$$D_{min} = L_{jstop} - L_{istop} + L_{safe}. \tag{8}$$

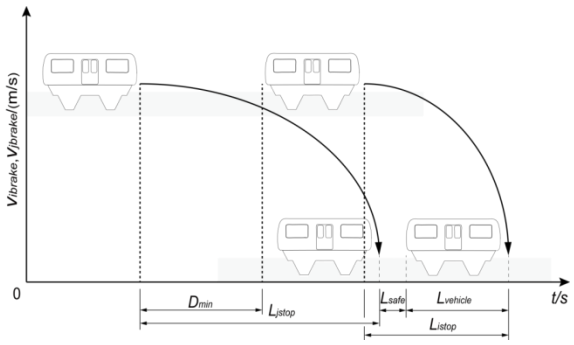

Fig. 3 The operation protection strategy of formation vehicles

The minimum safe tracking distance for vehicles considering the effect of slope is:

$$D_{min} = v_{jbrake}t_{jfree} + \frac{v_{jbrake}^2}{2(a_{je} + a_{jground})} - v_{ibrake}t_{ifree} - \frac{v_{ibrake}^2}{2(a_{ie} + a_{iground})} + L_{safe}, \tag{9}$$

where: v_{ibrake} and v_{jbrake} are the speeds of the front and rear vehicles when braking; t_{ifree} and t_{jfree} are the braking idling times of the front and rear vehicles, respectively; a_{ie} and a_{je} are the emergency braking accelerations of the front and rear vehicles; $a_{igruond}$ and $a_{jground}$ are the accelerations generated by the slope of the line where the front and rear vehicles are located, respectively.

Ultimately, the distance between formation vehicles operating in IFOM needs to be larger than the minimum safe tracking distance, which can be expressed as:

$$D_{vij} < D_{v\min ij}, \tag{10}$$

where: D_{vij} and D_{vminij} are the driving distance and the minimum driving distance of adjacent vehicles, respectively.

3.3. Running stability

Since each vehicle in the formation may be in different curves, the stability of the vehicle passing curve should also be considered. The overturning coefficient is used to evaluate the running stability of the vehicle, which can be expressed as:

$$D_i = \frac{\Delta P_{vi}}{P_{vi}} = \frac{P_{vi2} - P_{vi1}}{P_{vi2} + P_{vi1}}. \tag{11}$$

In which P_{vi1} is the vertical force of the wheel at the load reduction side; P_{vi2} is the vertical force of the wheel on the load increase side. In order to ensure the stability of vehicle, we believe that the overturning coefficient should be less than 0.8.

3.4. Passenger comfort

Formation vehicles should not only consider the effect of formation control, but also need to meet the needs of passenger comfort. The differential value of longitudinal acceleration is used to evaluate the comfort of passengers, see

Eq. (12).

$$J_{vi} = \int \left| \frac{\mathrm{d}a}{\mathrm{d}t} \right| \mathrm{d}t, \tag{12}$$

where: J_{vi} is the differential value of longitudinal acceleration of each vehicle in the formation. According to the regulations of most subway manufacturing contracts in China, the impact rate is generally required to be less than 0.75 m/s^3.

4. Formation vehicle operation controller

4.1. Vehicle longitudinal dynamics model

The running resistance of straddle-type rapid transit vehicles can be divided into basic resistance and additional resistance. The basic resistance is composed of rolling resistance and air resistance, and the additional resistance is composed of ramp resistance, curve resistance, tunnel resistance and acceleration resistance.

The rolling resistance of straddle-type rapid transit vehicles can be expressed as:

$$F_f = Mgf + M\left(4F_{spre} + 2F_{wpre}\right) f, \tag{13}$$

where: F_f is the rolling resistance of the vehicle; M is the mass of the vehicle; g is the acceleration of gravity; f is the resistance coefficient of the track surface; F_{spre} and F_{wpre} are the preloads of the steering wheel and the stabilizing wheel, respectively.

The air resistance of a vehicle can be expressed as:

$$F_w = C_D A \rho v_w^2 / 2, \tag{14}$$

where: F_w is the air resistance of the vehicle; C_D is the air resistance coefficient; A is the cross-sectional area of the windward side of the vehicle; ρ is the air density; v_w is the relative speed between the vehicle and the wind.

The ramp resistance can be expressed as:

$$F_s = MgS_n, \tag{15}$$

where: F_s is the ramp resistance; S_n is the slope of the line where the vehicle is located.

When the vehicle enters the curve, the running wheel will have lateral friction, and the steering wheel and the stabilizing wheel will roll and slide with the track beam, resulting in the curve resistance. The curve resistance includes the curve resistance of the running wheel and the curve resistance of the horizontal wheel.

The curve resistance of the running wheel can be expressed as:

$$F_{r\alpha} = k_\alpha \alpha^2, \tag{16}$$

where: k_α is the cornering stiffness of the running wheel, and α is the cornering angle of the running wheel.

The curve resistance of the horizontal wheel can be expressed as:

$$F_{r\theta} = \left(M \frac{v^2}{r} cos\theta - Mgsin\theta \right) f, \tag{17}$$

where: $F_{r\theta}$ is the curve resistance of the horizontal wheel; v is the running speed of the vehicle; r is the rolling radius of the horizontal tire; θ is the super-elevation angle of the line where the vehicle is located.

Therefore, the curve resistance of the vehicle passing through the curve is:

$$F_r = F_{r\alpha} + F_{r\theta} = k_\alpha \alpha^2 + \left(M \frac{v^2}{r} cos\theta - Mgsin\theta \right) f. \tag{18}$$

The acceleration resistance can be expressed as:

$$F_a = \delta M \frac{\mathrm{d}a}{\mathrm{d}t}, \tag{19}$$

where: δ is the conversion factor of the vehicle rotating mass, and dv/dt is the acceleration of the vehicle.

The tunnel resistance can be expressed as:

$$F_t = 0.00013 L_t, \tag{20}$$

where: L_t is the tunnel length.

In summary, the total running resistance of the vehicle can be expressed as:

$$\sum F = F_f + F_w + F_s + F_r + F_a + F_t. \tag{21}$$

The traction force u required by the vehicle is:

$$u = Ma + \sum F. \tag{22}$$

4.2. Artificial potential field formation algorithm

The artificial potential field algorithm has a wide range of applications in formation operation. It has the advantages of small control calculation, fast response and good effect, and is suitable for the formation vehicle operation control scene in this study. According to the method provided in [7], $tanh(x)$ is used as the potential field function to control the relative position and relative velocity of the vehicle.

The required traction force of the vehicle can be expressed as:

$$u = k_1 tanh(x_i - x_j - d_{ij}) + k_2 tanh(v_i - v_j), \tag{23}$$

where: k_1 and k_2 are the control gain coefficients of displacement and velocity, x_i and x_j are the positions of the front and rear vehicles, v_i and v_j are the speeds of the front and rear vehicles, and d_{ij} is the desired distance between the front and rear vehicles, d_{ij} can be expressed as:

$$d_{ij} = d_{stop} + v_j t_s, \tag{24}$$

where: d_{stop} is the parking distance of formation vehicles.

Formation operation always aims to achieve the

convergence of spacing and speed, which can be expressed as:

$$\begin{cases} \lim\limits_{t\to t_k}(x_i - x_j) = d_{ij} \\ \lim\limits_{t\to t_k}(v_i - v_j) = 0 \end{cases}, \tag{25}$$

where: t_k is the maximum convergence time of formation stable operation. If t_k is too large, the formation cannot converge in a short time, which affects the efficiency of line operation.

In addition, the acceleration and deceleration of the vehicle also need to meet the comfort requirements, see Eq. (26).

$$a_{tmax} < a_j < a_{bmax}, \tag{26}$$

where: a_{tmax} and a_{bmax} are the maximum acceleration and maximum deceleration of the vehicle during normal operation, respectively.

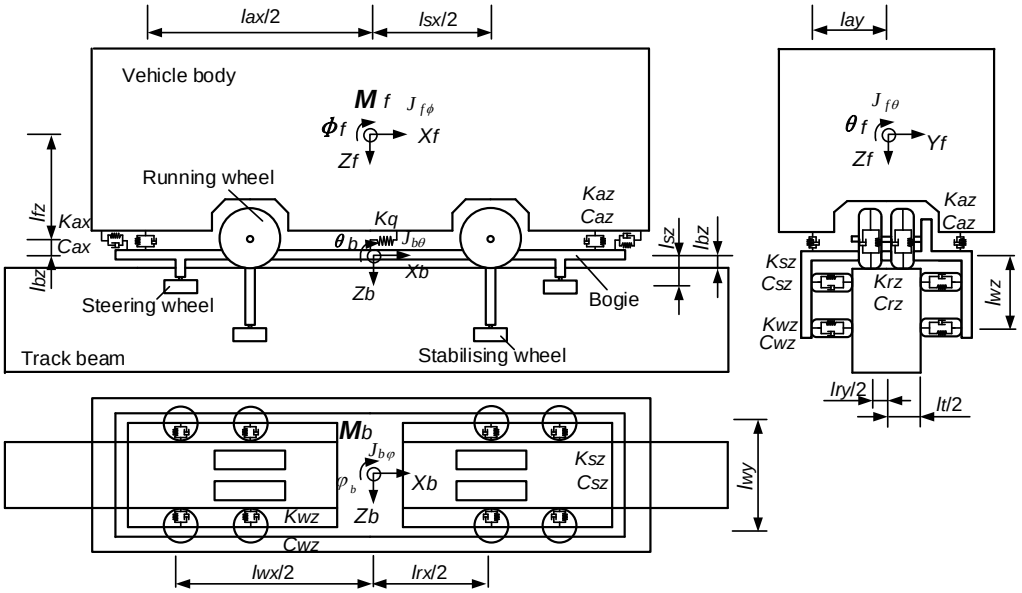

Fig. 4 Dynamics model of straddle-type rapid transit vehicle

5. Simulation model

5.1. Vehicle dynamics model

Fig. 4 shows the dynamic model of the new straddle-type rapid transit vehicle, which contains 12 degrees of freedom. The vertical and lateral motion of the vehicle can be expressed as:

$$M_f\ddot{Z}_f + 4k_{az}(Z_f - Z_b) + 4c_{az}(\dot{Z}_f - \dot{Z}_b) = 0, \tag{27}$$

$$\begin{aligned} &M_f\ddot{Y}_f + 4k_{ay}(Y_f - Y_b - \phi_f l_{fz} - \phi_b l_{bz}) + \\ &+4c_{ay}(\dot{Y}_f - \dot{Y}_b - \dot{\phi}_f l_{fz} - \dot{\phi}_b l_{bz}) = 0, \end{aligned} \tag{28}$$

where: M_f is the mass of the vehicle body; K_{az} and C_{az} are the vertical stiffness and damping of the secondary suspension; l_{fz} and l_{bz} are the height from the center of gravity of the vehicle to the secondary suspension and the height from the secondary suspension to the center of gravity of the bogie, respectively.

5.2. Multi rigid body dynamics simulation model of formation vehicles

The multi rigid body dynamics simulation model of the formation vehicle in the heterogeneous operating environment is shown in Fig. 5, which includes the vehicle power system and controller established in simulink, and the multi rigid body dynamics simulation model and opera-ting environment of formation vehicles established in simpack.

In simpack, different vehicle parameters are set for formation vehicles, and varying curves and slopes are set in the track. In simulink, not only a simple power system consisting of battery, motor and transmission system is built, but also a vehicle perception module consisting of V2V communication, radar and train ground communication (TWC).

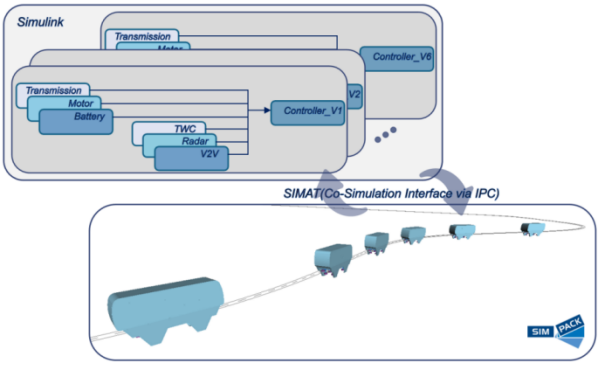

Fig. 5 Multi rigid body dynamics simulation model of formation vehicles

6. Simulation and analysis

6.1. Simulation scenario

In order to simulate the actual operation of formation vehicles, we set the initial speed of each vehicle to

zero. The speed curve of the leader vehicle adopts external input to simulate the running process of the formation starting from the station to stopping at the station. In addition, to simulate actual operating conditions, all three vehicles have different weights.

Due to the special construction process of straddle type monorail track beam, the running surface of the vehicle is different from that of other rail vehicles. According to laser scanning analysis and vehicle dynamic test, the running surface roughness is similar to Grade A specified in ISO 8606: 2016, so the running surface roughness in the model refers to the grade A road surface [10-11]. Besides, the delay of sensor and communication is not considered in the simulation.

6.2. Simulation results and analysis

The speed curves of formation vehicles and the speed difference between adjacent vehicles are shown in Figs. 6 and 7, respectively.

It can be seen that when the formation starts running, the following vehicle needs to accelerate to follow the preceding vehicle, and K_v gradually enlarges towards the rear of the formation. After that, the K_{v12} and K_{v23} curves tend to overlap, and the K_v curve changes smoothly. The positive and negative maximum values of K_{v12} are 0.21m/s and -0.39 m/s, which appear in the braking stage and the starting stage of the vehicle, respectively. The positive and negative maximum values of K_{v23} are 0.43 m/s and -1.15 m/s respectively, both of which appear in the starting stage of the vehicle.

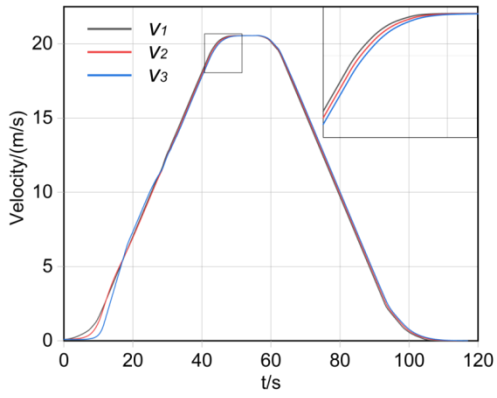

Fig. 6 Speed curve of formation vehicles

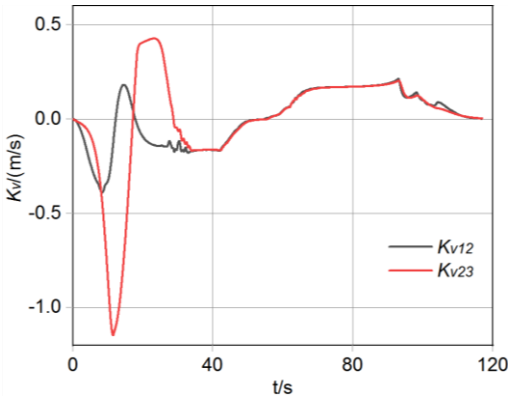

Fig. 7 Speed difference between adjacent vehicles

Fig. 8 is the longitudinal displacement curve of the vehicle, and Fig. 9 is the D_{vij} and D_{vminij} curves. It can be seen that the driving distance is greater than the minimum driving distance of adjacent vehicles. The maximum of D_{v12} is 10.4 meters, and the maximum of D_{v23} is 9.16 meters, which appear in the formation high-speed cruise stage and the starting stage respectively. This is because the formation is in the starting acceleration stage, the speed of the front vehicle becomes faster, and the rear vehicle is constrained by the acceleration, so D_{v23} becomes larger. After 30s, the distance between vehicles is propor-tional to the speed of the vehicle, which indicates that the longitudinal safety of the formation is excellent, and it also shows that the formation distance control effect is good.

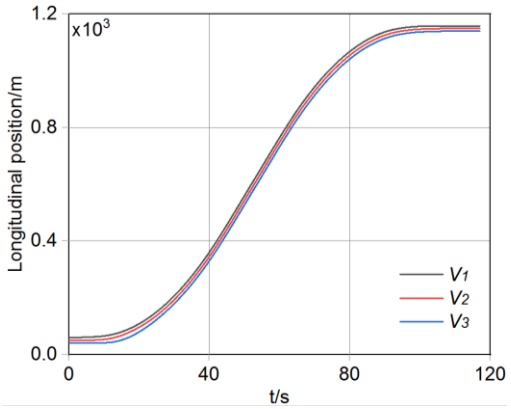

Fig. 8 Longitudinal displacement curve of vehicles

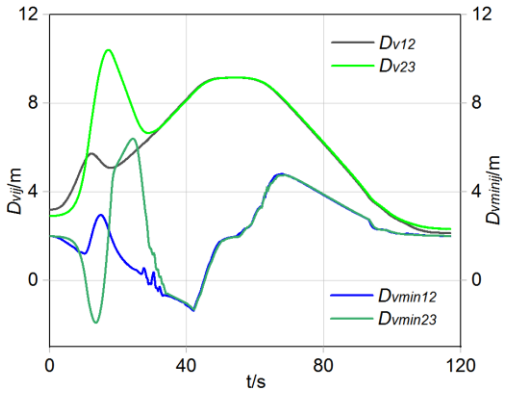

Fig. 9 D_{vij} and D_{vminij} curves

Fig. 10 is the overturn coefficient curve of formation vehicles.

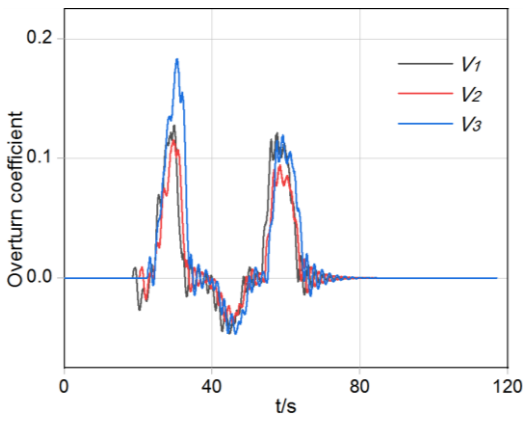

Fig. 10 Overturn coefficient curve of formation vehicles

The maximum values of the overturning coefficients of each vehicle are 0.128, 0.115 and 0.183, which all appear at the first curve of the line. Due to the difference in

the time and speed of the vehicle entering the curve, the driving stability of the vehicle through the curve is slightly different. However, it can be seen from Fig. 11 that the driving stability is independent of the formation position of the vehicles.

Fig. 11 is the longitudinal acceleration curve of formation vehicles, and Fig. 12 is the differential value of longitudinal acceleration curve of formation vehicles.

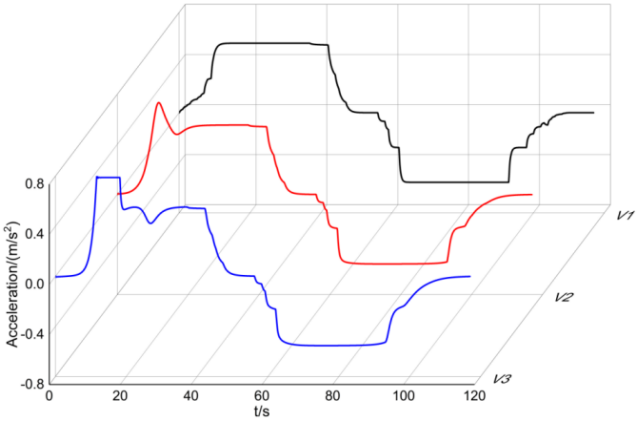

Fig. 11 Longitudinal acceleration curve of formation vehicles

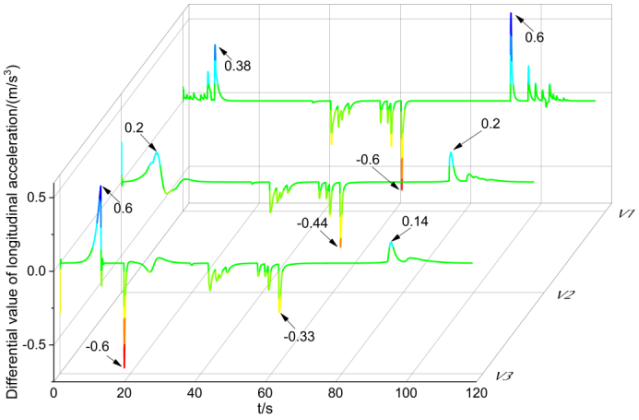

Fig. 12 The differential value of longitudinal acceleration curve of formation vehicles

It can be seen from Fig. 11 that the acceleration of the leading vehicle increases rapidly at the starting stage, while the acceleration of the following vehicle increases slowly. As the speed increases, the acceleration of the following vehicle gradually reaches the constraint value. After the formation stabilizes, the acceleration of the following vehicle is almost the same as that of the leading vehicle.

It can be seen from Fig. 12 that the maximum values of the differential value of longitudinal acceleration for each vehicle in the formation are 0.6 m/s^3, 0.44 m/s^3 and 0.6 m/s^3, which are all less than 0.75 m/s^3, which meets the passenger comfort requirements.

The maximum differential value of longitudinal acceleration of the leading car and the intermediate car is in the braking phase, and the last vehicle is in the starting phase, because the last vehicle needs to quickly catch up with the preceding vehicle when it starts.

Finally, we summarize the calculation results of the simulation, as shown in Table 1. It can be seen from the above simulation results that the K_v and D_v are far less than the index limit; the differential value of longitudinal acceleration is close to its index limit, but both meet the limit requirements. The D_{vij} curve is always higher than the D_{vminij} curve, which meets the requirements of vehicle operation protection. Therefore, we believe that the simulation results satisfy the evaluation index system of formation vehicle operation proposed in this paper.

Table 1

Calculation results of the simulation

Evaluation index	Simulation result	Index limit	Unit
$K_{v12max+}$	0.21	2	m/s
$K_{v12max-}$	-0.39	-3.14	m/s
$K_{v23max+}$	0.43	2	m/s
$K_{v23max-}$	-1.15	-3.14	m/s
D_{v1}	0.128	0.8	-
D_{v2}	0.115	0.8	-
D_{v3}	0.183	0.8	-
J_{v1}	0.6	0.75	m/s^3
J_{v2}	0.44	0.75	m/s^3
J_{v3}	0.6	0.75	m/s^3

7. Conclusion and outlook

This paper takes the straddle-type rapid transit vehicle using IFOM as the object, firstly defines the operation mode of the vehicle, and proposes the evaluation index system of the formation vehicle operation. Then, the formation vehicle operation controller and the multi rigid body dynamics simulation model in the heterogeneous operation environment are established. Finally, the operation performance of formation vehicles is analyzed, and it is found that the operation performance of formation vehicles meets the requirements of the evaluation index system, which proves the feasibility of formation operation of straddle-type rapid transit vehicles.

More importantly, we found that the multi rigid body dynamic model of vehicles can be solved simultaneously when controlling the operation simulation of vehicle formation. Therefore, the safety and comfort of the vehicle when passing the curve can also be included in the control objectives, so as to solve the optimal speed of each vehicle according to the real-time vehicle status and operating environment. In this way, not only the stable operation of vehicle formation is realized, but also the passengers of each vehicle can have a better riding experience.

Acknowledgement

This work is supported in part by Chongqing Postgraduate Scientific Research Innovation Project [grant number: CYB22238] and General Program of Chongqing Natural Science Foundation [grant number: CSTB2022-NSCQ-MSX1264].

References

1. **Haoxin, W.; Zixue, D.; Zhen, Y;** et al. 2022. Coordination and matching of tire system of new straddle-type rapid transit vehicle [online] Vehicle System Dynamics [accessed 4 Mar. 2022]. Available from Internet: https://doi.org/10.1080/00423114.2022.2051568.
2. **Bock, U.; Bikker, G.** 2000. Design and development of a future freight train concept-virtually coupled train formations, IFAC Proceedings 33(9): 395-400.

https://doi.org/10.1016/S1474-6670(17)38176-4.
3. **Xun, J.; Chen, M.; Liu, Y.; Liu, F.** 2020. An over speed protection mechanism for virtual coupling in railway, IEEE Access 8: 187400-187410. https://doi.org/10.1109/access.2020.3029147.
4. **Felez, J.; Kim, Y.; Borrelli, F.** 2019. A model predictive control approach for virtual coupling in railways, IEEE Transactions on Intelligent Transportation Systems 20(7): 2728-2739. https://doi.org/10.1109/tits.2019.2914910.
5. **She, J.; Li, K.; Yuan, L.;** et al. 2020. Cruising control approach for virtually coupled train set based on model predictive control, New York, IEEE 23rd International Conference on Intelligent Transportation Systems 1-6. https://doi.org/10.1109/itsc45102.2020.9294534.
6. **Wang, H.; Zhao, Q.; Lin, S.;** et al. 2020. A reinforcement learning empowered cooperative control approach for IIoT-based virtually coupled train sets, IEEE Transactions on Industrial Informatics 17(7): 4935-4945. https://doi.org/10.1109/tii.2020.3024946.
7. **Qianqian, Z.** 2021. A Multi-Train Cooperative formation method based on reinforcement learning. Beijing Jiaotong University, China. https://doi.org/10.26944/d.cnki.gbfju.2021.002573.
8. **Jiangfeng, S.** 2021. A centralized control method for virtually coupled train set based on model predictive control, Beijing Jiaotong University, China. https://doi.org/10.26944/d.cnki.gbfju.2021.002999.
9. **Junchao, Z.; Zixue, D.; Zhen, Y.;** et al. 2020. Dynamic parameters optimization of straddle type monorail vehicles based multi-objective collaborative optimization algorithm, Vehicle System Dynamics 58(3): 357-376. https://doi.org/10.1080/00423114.2019.1578384.
10. **Junchao, Z.; Zixue, D.; Zhen, Y.;** et al. 2019. Dynamics study of straddle-type monorail vehicle with single-axle bogies-based full-scale rigid-flexible coupling dynamic model, IEEE Access 7: 110249-110257. https://doi.org/10.1109/ACCESS.2019.2933991.
11. Mechanical vibration - Road surface profiles - Reporting of measured data. ISO 8608-2016. International Organization for Standardization, 2016.

Z. Du, H. Wu, Z. Yang, X. Wen

RESEARCH ON INTELLIGENT FORMATION OPERATION PERFORMANCE OF STRADDLE-TYPE RAPID TRANSIT VEHICLES IN HETEROGENEOUS OPERATING ENVIRONMENT

S u m m a r y

This paper presents an intelligent formation operation mode (IFOM) based on straddle-type rapid transit vehicles. Taking the straddle-type rapid transit vehicles operating in IFOM as the object, the operation mode of the vehicle is defined in the control system architecture of the straddle-type rapid transit system. In addition, considering the heterogeneous operating environment of formation vehicles, an evaluation index system for formation vehicles is proposed. Then, according to the vehicle longitudinal dynamics model and the artificial potential field formation algorithm, we build the formation vehicle operation controller. After that, referring to the vehicle dynamics model, a multi rigid body dynamics simulation model of formation vehicles in a heterogeneous operating environment is established. Finally, the operating performance of formation vehicles in heterogeneous operating environment is analyzed. The analysis results show that the operation performance of the formation vehicle meets the requirements of the evaluation index system, which proves the feasibility of the formation operation of straddle-type rapid transit vehicles operating in IFOM.

Keywords: straddle-type monorail, rapid transit vehicle, multi-body dynamics, vehicle formation operation, formation control algorithm.

Received August 20, 2022
Accepted January 27, 2023